

Nanocrystalline Ni-W Alloy Coating for Engineering Applications

A.R.Jones,*¹ J. Hamann,¹ A.C. Lund¹ and C.A. Schuh²

¹Xtalic Corporation, Marlborough MA, USA

²Department of Materials Science and Engineering, Massachusetts Institute of Technology, Cambridge MA, USA

This paper describes a newly-developed nanocrystalline Ni-W alloy coating with both excellent corrosion and wear resistance as compared to other commercially available electroplated coatings. This technology employs unique chemistry and applied current waveforms to control precisely grain structures at nanometer length scales (2 to 200 nm). The resulting coatings are structurally stabilized, and resist grain growth and associated softening as often seen with other traditional (e.g., hard chromium) or nanocrystalline engineering coatings. Further, unlike coatings such as electroless Ni-P, nanocrystalline Ni-W can be further hardened via baking without compromising other performance metrics, making it a candidate for application at modestly elevated temperatures (up to ~300°C). Additional important performance attributes include improved thickness distribution and significantly less surface roughness after plating, which permit reduced plating times and less post grinding.

Keywords: Nickel-tungsten alloy, alloy plating, nanocrystalline, wear, corrosion, engineering coatings, pulse reverse electrodeposition

Introduction

“Engineering” or “functional” coatings are broadly employed commercially to provide enhanced surface performance for engineering components. Typically wear and corrosion resistance are the two critical properties for an engineering coating, with secondary considerations including surface finish, coefficient of friction, surface coverage and throwing power. The most common and well-known functional coating is hard or functional chromium (hard Cr),^{1,2} the properties of which are often used as a standard benchmark for other engineering coatings.

In recent decades much effort has been spent looking at alternatives to electroplated hard chromium. This effort has been driven by a combination of environmental and worker safety concerns surrounding the hexavalent Cr(VI)-based plating process, and a desire for better-performing coatings for many applications. Some proposed hard chromium alternatives, including thermal or plasma sprayed coatings,³⁻⁶ vapor-deposited coatings,^{7,8} and electroless Ni-

P (EN) coatings,⁹ have found use in select applications. While each of these competing technologies offers some important benefits, each has also been restricted in its scope of application by fundamental limits of the technology. Such limits include the line-of-sight nature of spray technologies, the need for highly-engineered environmental cabinets for vapor deposition, and the tradeoff between heat-treat hardening vs. cracking and loss of corrosion protection in EN.

Another class of coatings that has been considered as a hard chromium alternative is electrodeposited nanocrystalline coatings, and in particular nickel- or cobalt-based nanocrystalline materials. While these coatings have found some interesting niche applications, they have not yet achieved broad application. Unalloyed nanocrystalline coatings coarsen very quickly,¹⁰⁻¹³ and thermal stability is often achieved through alloying. A variety of electroplated nanocrystalline alloys have been demonstrated in the scientific literature,¹⁴⁻¹⁹ but these have not yet found significant commercial success as functional or engineering coatings. The most common alloying elements for the nickel- or cobalt-based alloys are metalloids such as boron or phosphorus (which can often cause embrittlement or cracking), or other transition metals such as iron, tungsten or molybdenum.

One such nanocrystalline alloy, Ni-W, has been studied regularly since the seminal work of Brenner,^{20,21} and shows particular promise as an engineering coating. Recent advances in characterization of nanocrystalline Ni-W alloys have revealed in detail the connections between processing, composition, structure and properties of these alloys.²²⁻³¹ As a result of this activity, Detor and Schuh,^{30,32,33} were able to propose new processing strategies to broaden significantly the properties accessible in the Ni-W alloy system through the use of pulse-reverse electrodeposition.

* Corresponding author:
Allen R. Jones, Ph.D.
Xtalic Corporation
260 Cedar Hill Street
Marlborough, MA 01752 USA
Phone: (508) 485-9730
E-mail: ajones@xtalic.com

In this paper we discuss a potential alternative to hard chromium developed by the current authors, which takes advantage of these new processing techniques in the Ni-W system. Specifically, we report on the benefits that this approach offers in regard to critical performance metrics. Because the plating process is free of hexavalent chromium, it also enjoys a substantially reduced environmental and worker health and safety footprint as compared to hard chromium electroplating.

Experimental methods

The proprietary coating** we describe herein, which we refer to as "XP" for convenience, is produced using a tailored pulse-reverse waveform combined with an appropriate chemistry to produce an engineered coating with optimized properties. The plating technique includes a repeated sequence of forward and reverse current pulses, and employs an optimized proprietary chemistry that is an advancement of the classic Brenner bath²¹ for electroplating of Ni-W alloys. Some details of the bath make-up are provided in Table 1. Further details of the processing method are not provided here as they are proprietary in nature.

For the series of experiments reported here, a Power-Pulse (pe86C-15-27-27-S) rectifier from Plating Electronic GmbH (Denzlingen, Germany) was used, with plating control software from TCD Teknologi ApS (Copenhagen, Denmark). Electrodeposition was conducted in an 85-L polypropylene tank equipped with an immersion pump, heater, temperature probe and pH probe. Inert anodes (AISI 316) were used with an anode-to-cathode distance of ~18 cm. Several different types of specimens were prepared, as described in the following sections. In some cases, identical substrates were plated with the XP coating, hard chromium (high efficiency non-fluoride process) and EN (high phosphorus, unbaked). The latter two coatings were applied by a third party electroplater, and were prepared to provide a direct comparison of the properties of XP with these conventional engineering coatings.

Wear testing

The substrate coupons used for wear testing were plain steel disks (AISI 1030 grade, 51 mm diameter, 3.2 mm thick) metallurgically polished through a 0.3 μm SiO₂ slurry to achieve a flat surface finish. XP coatings were plated to a thickness of 15 μm , while the hard chromium and EN coatings were approximately 25 μm thick.

Sliding wear resistance was assessed using conventional pin-on-disk (POD) testing, using a Ball-on-Disk/Pin-on-Disk Tribometer (TRB-S-DU-0000) from CSM Instruments (Needham, MA, USA), operating in a rotational mode. A 6-mm diameter WC sphere was used as the counterbody. Prior to each test, the rotational velocity, friction force and rotating diameter of the POD apparatus were calibrated. Immediately prior to testing, the plated disk and WC counterbody were wiped with acetone and dried with forced air to ensure a clean contact. The rotational velocity of the plated sample for each test was 15 cm/sec, the wear track diameter was held constant at 10 mm, and the test duration was 8,000 cycles. For both XP and hard chromium, the applied normal load employed in testing was 3 N, whereas for EN it was necessary to reduce the applied load to 1 N. This will be discussed in more detail later.

** XPROTECT™, Xtallic Corporation, Marlborough, MA, USA.

Table 1
Chemistry and deposition conditions

	Operating value	Range
Ni, g/L	6.5	6 - 7
W, g/L	32.5	29 - 36
Additives	Yes	
pH	7.9	7.7 - 8.1
Plating rate, $\mu\text{m/hr}$		30 - 40
Temperature, °C	60	58 - 62

Following POD testing, the profiles of the wear tracks were mapped using a P10 profilometer from KLA-Tencor (Milpitas, CA, USA) equipped with a 2- μm radius stylus. Based on the profilometry scans, the volumetric wear rates of the coating were calculated.

Corrosion testing

The substrates used for corrosion testing were hardened precision ground shafts of AISI 1566 steel (part #6061K12 from McMaster-Carr, Atlanta, GA, USA), 15 cm long with a diameter of 0.95 cm. Prior to plating, the rods were cleaned and then activated by immersion in hydrochloric acid. The area ratio between anode and cathode for plating these specimens with XP was 4:1, and XP coatings of several thicknesses were prepared: 12, 18 and 25 μm .

For comparison, the same substrate shafts coated with hard chromium (part #60345K21 from McMaster-Carr) were also acquired. These rods were post-finished by the manufacturer, had a nominal hard chromium coating thickness of 12 μm , and were 15 cm long with a diameter of 1.27 cm. The hard chromium coatings on these rods were specified to conform to AMS 2460, Class 1 (Corrosion Protective Plating), Type 1 (Bright finish) according to the supplier.

Standard neutral salt spray (NSS) testing was performed in a SCCH21 cabinet from Singleton (Cleveland, OH, USA) according to ASTM B117.³⁴ The hard chromium samples were tested in the as-received condition, while the XP samples were tested in the as-plated condition without post-finishing. We evaluated corrosion protection using two performance metrics based on the NSS test. The first metric defined the failure time at the first appearance of red rust, which is indicative of the onset of substrate corrosion. This is a stringent test criterion, as any individual flaw on the surface is logged as a failure of the specimen as a whole. An alternative rating scale is provided by ASTM 537,³⁵ where a relative rating of 10 indicates no corrosion, a rating of 9 denotes 0.1% of the specimen surface area has corroded, etc. This rating was used primarily as a means of evaluating the severity of the failures seen using the more stringent metric. Samples were usually removed from the test after the first sign of corrosion, so generally no ongoing rating was calculated after the first failure.

Surface finish

Profilometry (surface finish) data was obtained using a Surtronic 25 (K505/125E-01) from Taylor-Hobson Ltd (Leicester, England, UK). Three characteristic roughness measurements were made: R_a is the arithmetic average of the absolute values of the vertical deviations in the surface, R_t is the total roughness (the maximum peak-to-valley differential), and R_c is an average peak-to-valley differential measurement.

Thickness distribution

To explore the distribution of the XP coating thickness, two substrate geometries were used. The first was the same 1566 steel shaft described above in reference to the corrosion testing. For this geometry, plating was conducted with an anode-to-cathode area ratio of 5.3:1. The second substrate was a spur gear (part #1L959 from McMaster-Carr) with the following dimensions: outer diameter 4.19 cm, hub diameter 3.02 cm, face width 1.27 cm, with a pitch of 16. For plating this sample an anode-to-cathode area ratio of approximately 8:1 was used. For the gear, coating thickness was assessed through cross-sectional metallography using either an optical microscope or a scanning electron microscope (SEM, LEO 1430VP) from Carl Zeiss SMT Inc. (Peabody, MA, USA). For the shafts, thickness data were obtained using x-ray fluorescence (XRF) measurements made using a Fischerscope (XDL-XYZp) from Fischer Technology Inc. (Windsor, CT, USA).

Results and discussion

Sliding wear resistance

Profilometry results showing typical cross-sections of the POD wear tracks for each coating are shown in Fig. 1, and calculated wear rates are listed in Table 2. The striking feature captured by these data is the order-of-magnitude difference in wear rate between the XP coating and hard chromium, and the more than two orders-of-magnitude improvement of XP over EN. It is interesting that there is such a large difference between XP and EN despite the significantly gentler test conditions applied for EN. As already noted in the procedure section, EN was run with a 1 N load compared to the 3 N load used for XP and hard chromium; this change was necessary because the compliance and wear of EN at a 3 N load led to an overload condition on the POD instrument. Were the instrument able to perform the test at a 3 N load, the wear rate of EN would be significantly higher than that reflected in Fig. 1 and Table 2, and the relative advantage of XP even higher.

Optical micrographs of the wear tracks (top-down view) are presented in Fig. 2. These images corroborate the track widths measured by profilometry. Not reflected in these images are subtle differences in the wear process among these samples. Specifically, the center of the wear track on the hard chromium coated sample exhibited a fine crack network, whereas the XP and EN wear tracks did not exhibit any cracks.

Corrosion resistance

The results of the corrosion testing are shown in Fig. 3 for XP coating thicknesses of 12, 18 and 25 μm , and hard chromium coatings of 12 μm thickness. Figure 3 presents the fraction of samples that did not exhibit any corrosion spots, as a function of NSS exposure. For the XP coating, the majority of samples exhibited no red rust corrosion sites after 1000 hr. Half of the samples of 18 μm thickness exceeded 3600 hr of exposure, as denoted by the run-out arrow on Fig. 3. This result reveals the intrinsic corrosion protection of the coating, in the absence of specific local defects. Figure 4 presents photographs that show the 12- μm XP-coated samples after corrosion testing. When a red rust corrosion site appeared,

it was typically very small (sub-mm) and below the resolution of the photographs shown here. The corrosion ratings collected for some of the failed specimens in Table 3 support the small size of the corrosion sites.

Also shown in Fig. 3 is data for equivalent testing of 12- μm thick hard chromium deposits on the same steel substrate material. As mentioned above, these shafts were acquired in a post-finished condition. Post-finishing typically increases the corrosion resistance of hard chromium. However, all of the hard chromium shafts tested here exhibited red rust corrosion sites after 2 hr of NSS exposure. After 4 and 48 hr there were approximately 7 and 300 corrosion sites/ cm^2 , respectively. These numbers are translated into the rating data provided in Table 3. Photographs of the chromium-plated shafts after 48 hr of NSS exposure are shown in Fig. 5, where it can be seen that at this thickness and test duration, the amount of corrosion is extreme.

Table 2

Total penetration depths after 8000 cycles and volume wear rates for the XP coating, hard chromium and EN

Coating	Load [N]	Penetration depth [μm]	Wear rate [mm^3/hr]
XP	3	0.2	1.0×10^{-3}
XP, 400°C/4 hr	3	0.1	4.0×10^{-4}
Hard Cr	3	1.5	2.3×10^{-2}
EN	1	10.5	2.9×10^{-1}

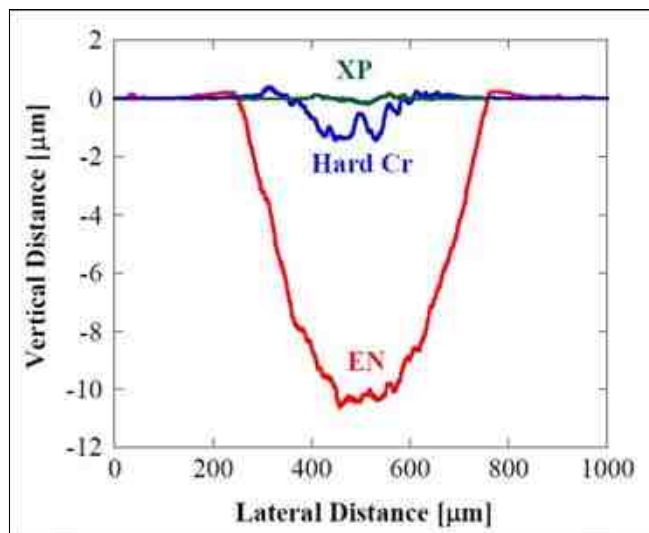


Figure 1—Two-dimensional profilometer scans of POD wear tracks on XP, EN, and hard chromium coatings deposited onto a plain steel substrate. XP and hard chromium coatings were tested with a higher applied load (3 N) than the EN coating (1 N).

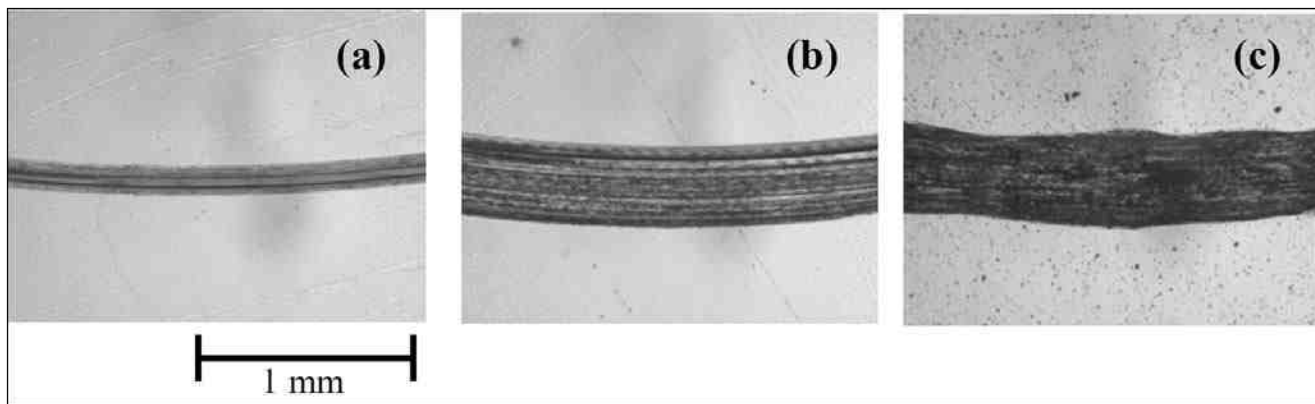


Figure 2—Light optical micrographs of the POD wear tracks on (a) XP, (b) hard chromium and (c) EN.

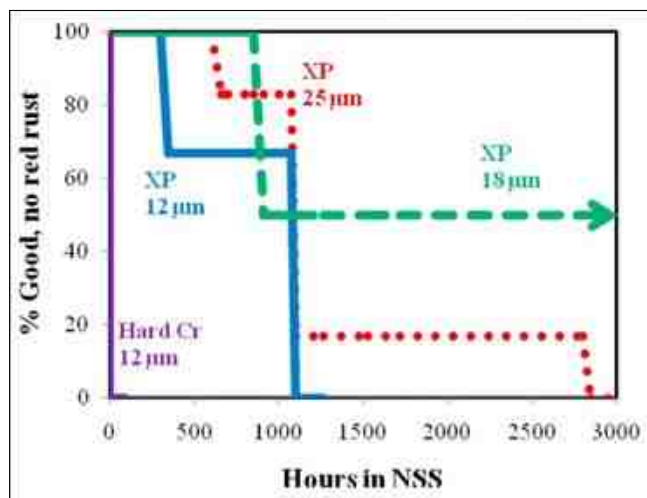


Figure 3—NSS corrosion resistance for various coatings plated on steel shafts. Performance for 12 μm hard chromium coating and XP coatings of different thicknesses are shown; the hard chromium specimens all failed in less than two hours.

The results reported here for corrosion resistance of hard chromium are consistent with generally accepted values.³⁶⁻³⁹ For example, coatings 35-μm thick are reported to offer between 24 and 122 hr in NSS testing, depending on the pretreatment process. The corrosion performance shown here by the XP coating is substantially superior to either the tested or literature-reported values seen or expected for hard chromium.

It is interesting in this context to also compare to typical corrosion resistance for EN, which is sometimes used in place of hard chromium for its superior performance in NSS. Literature values for NSS corrosion resistance of EN over plain carbon steels are summarized in Table 4,⁴⁰ where it can be seen that EN performance is substantially affected by phosphorus content in the plated alloy. At high phosphorus levels the corrosion performance is improved.

The data reported above are for as-plated EN, which lacks good wear performance (cf. Fig. 1). With heat treatment the hardness and wear performance can be improved. For example, an EN deposit with 10.5% P has an as-deposited HV_{100g} of 480 and a post-heat treatment (290°C for 6 hr) HV_{100g} of 900.⁹ However, in this same paper the authors report that the heat treatment reduces the corrosion resistance in 10% HCl by a factor of 126. This is a characteristic result for EN, where corrosion resistance and wear performance tend to be inversely correlated.

Table 3

Average corrosion resistance rating (based on ASTM 537³⁵) for XP coatings of different thicknesses, in comparison to hard chromium. Samples were plated on steel shafts, XP-coated samples were tested as-plated, while hard chromium-coated samples were post-finished prior to testing.

XP			Hard Cr		
Thickness [μm]	Hours	Rating	Thickness [μm]	Hours	Rating
12	353	9.8	12	4	8
-	-	-	12	48	1
18	910	9.1	-	-	-
25	664	9.8	-	-	-

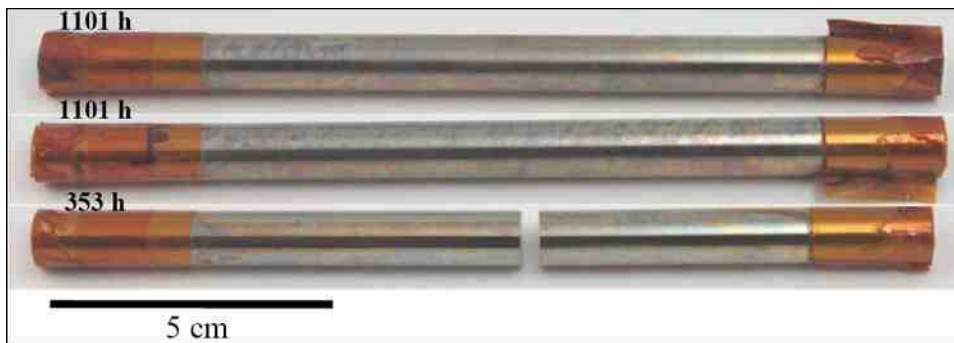


Figure 4—Appearance of 12- μm XP-coated steel shafts after exposure to NSS, with exposure times as shown. The ends of these shafts are masked (orange) during testing.

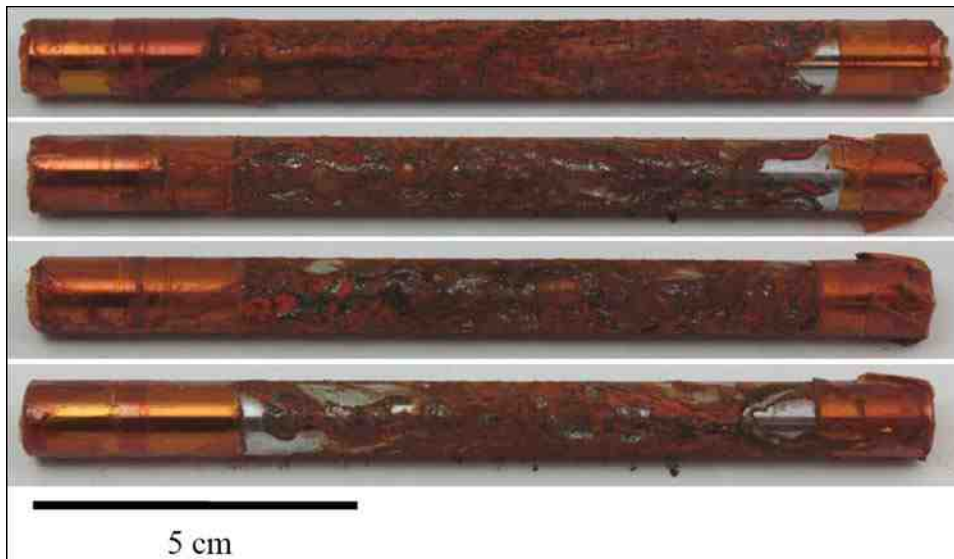


Figure 5—Appearance of 12- μm hard chromium coated steel shafts after 48 hr of exposure to NSS. The ends of these shafts are masked (orange) during testing.

Table 4
Neutral salt spray corrosion resistance rating for EN coatings⁴⁰

Thickness [μm]	Hours in NSST	
	4.0 - 8.0% P	10.5 -12.0% P
12	24	250
22 to 50	96	1000

Surface texture

Figure 6 shows the measured R_a roughness of coated substrates as a function of the initial substrate roughness. The data for hard chromium are taken from the literature,³⁷ and show an increase in roughness with thickness. On the other hand, XP coatings roughen the surface substantially less. For substrates with the same starting surface finish (0.12 μm), a 50- μm hard chromium deposit increased the substrate R_a value by about 90% while 25- or 100- μm XP coatings will increase the surface roughness of the substrate by

only 40 or 67%, respectively. Further, when the starting substrate is rougher, the XP coating can in some cases decrease the surface roughness after plating. For example, for a starting substrate R_a of 1.1 μm , the roughness change for a 25- or 100- μm XP coating is -32 or -14%, respectively.

A negative change in the R_a indicates that leveling has occurred during the plating process. Leveling is not observed for very smooth substrates because the intrinsic texture of the coating is more significant than the substrate roughness. In other words, there is some maximum degree of smoothness that is reached in the as-deposited coating.^{***} This is more clearly demonstrated in Fig. 7, where it can be seen that the roughness parameters decrease for a 25- μm thick XP deposit. For a 100- μm thick XP coating, R_t has only a slight increase and little to no change is seen in R_z or R_a from the unplated surface.

The data in Figs. 6 and 7 demonstrate that the XP coating can better replicate the surface finish of the substrate than a hard chromium coating. In some cases, the XP coating can actually level the substrate providing a smoother finished surface. This could provide an advantage in manufacturing, allowing the degree of post-finish-

^{***} The degree of leveling reported here is for the standard XP plating chemistry. This can be further controlled through adjustments of the bath chemistry if desirable.

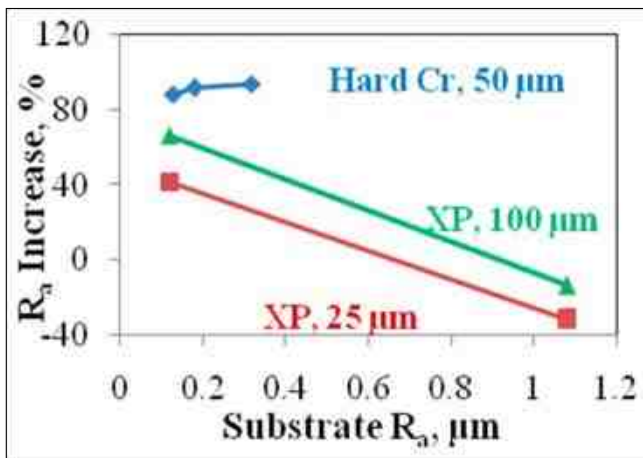


Figure 6—Surface roughness increase versus substrate roughness for XP and hard chromium deposits.

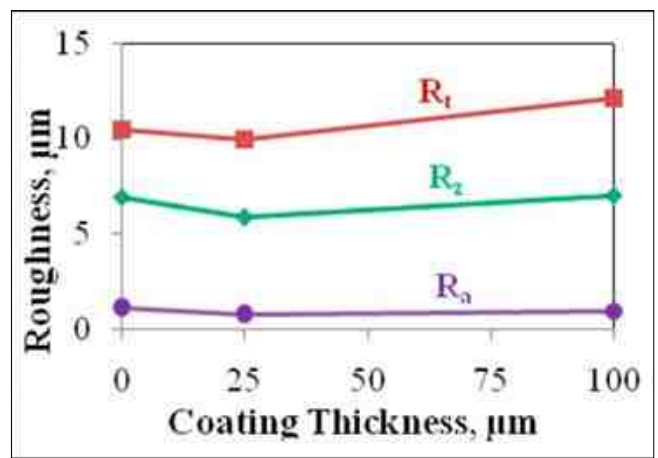


Figure 7—Surface roughness parameters versus XP coating thickness.

ing to be partially, or in some cases fully, eliminated. XP samples plated onto substrates of initial $R_a = 0.12 \mu\text{m}$ are shown in Figs. 8(a) and (b). In Fig. 8(a), for a 25- μm thick coating the substrate grind lines are visible (and indicated by arrows), whereas in Fig. 8(b), they are virtually leveled out. The small nodules shown in Figs. 8(a) and (b) are about 5 and 25 μm in diameter for coating thicknesses of 25 and 100 μm , respectively. On the other hand, a hard chromium deposit³⁸ that is 25 μm thick has nodules that are about 35 μm in diameter.

Coating distribution

Another factor that can substantially impact the degree of post-processing necessary after plating is the coating distribution. If substantial differences are seen in the relative plated thicknesses in higher and lower current density areas, it is more likely that a part will need to be post-machined to achieve desired tolerances. Typical processing issues include excessive build-up on gear teeth or “dog-boning” of shafts and plates.³⁹ The two geometries selected for the present experiments specifically address these two conditions. It is important to note that for these experiments, no special anode configuration was used. Flat anode sheets were simply positioned on either side of the substrates, without thieves or shields.

A photo of a plated gear (details of the gear are provided in the Experimental methods section) is provided in Fig. 9, along with cross-sectional micrographs showing the plating distribution. The peak-to-valley ratio for the XP coating thickness is approximately 4:1. The XP coating is also very smooth along the peaks of the teeth, with no substantial edge build up on the edges. By contrast, hard chromium processes typically exhibit poor covering power.³⁹ For the present geometry, one would typically expect no better than a 10:1 peak-to-valley distribution for hard chromium, and in some cases no coating at all would be expected in similar recesses. A closer comparison to what is shown in Fig. 9 would be to expectations for standard commercial nickel, the throwing power of which is accepted to be much superior to that of hard chromium.

Thickness distributions of the XP coatings were also measured on the same shafts used for the corrosion and surface roughness measurements. The results of these measurements are shown in Fig. 10. Two separate shafts were measured, with two sets of measurements taken on opposite sides of each shaft at 14 evenly spaced points. In general, all the measurements taken were within the noise of the measurement ($\pm 2 \mu\text{m}$), with only one data series showing a thickness increase significantly beyond the noise in the measurement at one end of the shaft. This maximum increase was minimal,

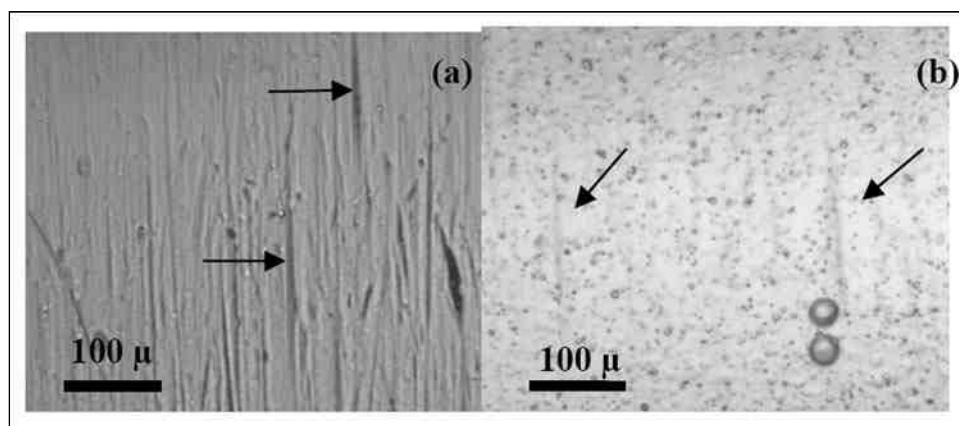


Figure 8—Optical micrographs of XP-coated surface appearance of samples from the roughness testing (see Fig. 7). The substrates were steel shafts with an R_a of 0.12 μm . The XP coating thickness is 25 μm in (a) and 100 μm in (b).

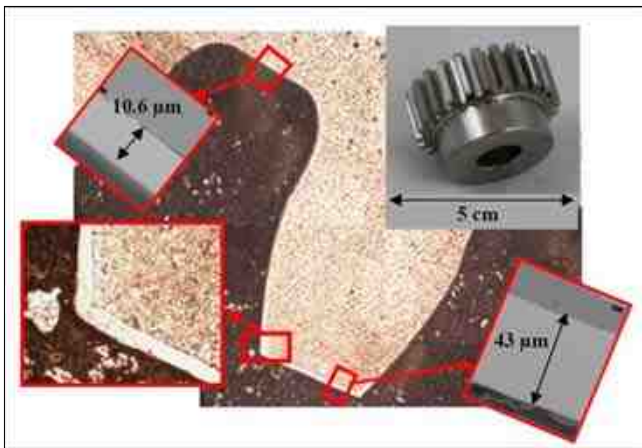


Figure 9—XP coating distribution on a spur gear. No special fixturing was used for the plating of this gear. The peak to valley coating thickness ratio is 4:1.

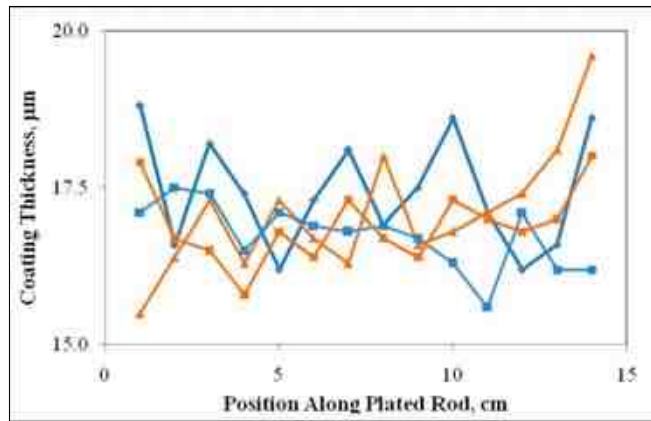


Figure 10—Distribution of XP coating on two 1566 shafts, with the two different shafts represented by different colors. The two series shown for each shaft are reflective of measurements taken on opposite sides of the respective shafts.

being only about 6%, and the next highest variation was only about 3%. These measurements were all within the measurement precision with no notable trends to higher thickness towards the ends of the shafts, suggesting that dog-boning should be minimal when using the XP coating process.

Heat treatment

Mild heat treatments of nanocrystalline Ni-W coatings are known to increase their hardness, by virtue of relaxation of the grain boundaries.⁴¹ For the present XP coating, a bake at 191°C for six or more hours increases the microhardness to 950 HV_{100g} without causing macrocracks in the coating. This is shown in the photomicrograph in Fig. 11. The ability to bake-harden without cracking is in contrast to many phosphorus-containing electrodeposits that crack under such treatments. Heat treatment can also be used to further improve wear resistance, as shown in Table 2, where a 4-hr treatment at 400°C roughly halves the wear rate.



Figure 11—Cross-sectional photomicrograph of an XP coating over steel, after a 191°C bake for 24 hr. Note the absence of cracks.

Application example

The wear and corrosion benefits of the XP coating lend it to industrial uses with high durability requirements. Here we present one in-service application test that validates these properties. The specific application is in the field of gravure printing, wherein a rotating disk with embossed letters on its outer circumference is used to transfer ink to a travelling medium. On each revolution the embossed letters are exposed to an ink, and experience mechanical contact wear as they are impressed into the medium. In the present test a wire-printing gravure wheel was selected for validation of the XP coating. A photograph of a similar such gravure wheel is shown in Fig. 12. The wheel diameter is 8.2 cm, and its thickness is 0.9 cm.

The performance of the coating is measured in terms of the length of printed wire that can be obtained before wear renders the printed letter quality unacceptable. Such wheels, when coated with commercial hard chromium, exhibit a typical lifetime of 13.5 km. A wheel was coated with 12 μm of the XP coating, and placed into industrial service. It delivered more than 135 km of printed wire without failing. This result aligns well with the relative improvements in wear vis-à-vis hard chromium observed in our laboratory tests.



Figure 12—Photo of a commercial gravure wheel coated with the XP coating. The embossed letters on the outside diameter, which comprise the functional surface, can be seen on the bottom of the photograph (as highlighted by the arrow).

Conclusions

While nanocrystalline electrodeposits have been proposed as hard chromium alternatives in the past, these have all suffered from drawbacks in terms of performance or stability of their structure or properties. Nanocrystalline Ni-W is unique in the sense that it is based on an alloy of two transition metals and has a broadly tunable structure and property set. The XP coating explored in this work represents an optimized coating intended for use in functional or engineering applications.

Our pin-on-disk sliding wear tests show that XP coatings have a significantly slower wear rate than either hard chromium (by a factor of 7.5 by depth) or electroless nickel (by a factor of more than 52 by depth). Compared with hard chromium, wear leads to less associated cracking, while in comparison to EN, improved wear properties are delivered without the need for heat treatment.

The neutral salt spray corrosion resistance of XP-coated steel shafts is significantly better than that attained with hard chromium plating. Even significantly thinner deposits of the XP coating can provide corrosion resistance equal to or surpassing thicker chromium deposits. The corrosion resistance of XP-coated steel is also comparable to or better than an equivalent thickness of EN.

XP coatings can replicate the surface texture of the substrate or, in some cases, can even improve the surface finish of the part. This attribute can reduce post-finishing costs, and may even allow polishing of the substrate before plating, rather than post-plating polishing of the coated component (as is common in hard chromium plating). The ability of the XP process to throw into recesses also offers many advantages when compared to chromium plating. It permits shorter plating times when a recessed area requires a minimum deposit thickness. Lower edge build-up on sharp corners is a peripheral benefit that can result in less post-finishing of the part.

Although as-plated XP coatings exhibit all of the desirable properties noted above, they can also be hardened through heat treatment. At lower bake temperatures than are common for EN, the wear resistance of XP coatings can be doubled. Cracks are not formed in XP coatings after baking, suggesting that high hardness, wear resistance and corrosion protection can all be simultaneously achieved in XP coatings with appropriate plating and baking cycles.

Nanocrystalline Ni-W alloy coatings are very well suited for engineering applications that require excellent wear and corrosion performance, and its deposition attributes offer significant production efficiencies. Here we have provided just one application example that validates the properties seen in our laboratory experiments. XP-coated gravure printing wheels exhibit an in-service lifetime more than ten times that delivered by commercial hard chromium.

Acknowledgements

The authors would like to thank the following other Xtallic employees for their assistance in the sample preparation, testing and analysis of data for this article: Don Baskin, Miranda Gray, Matt Little and Darci Silva.

References

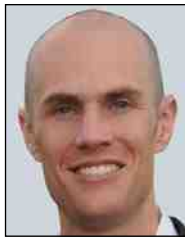
1. J.K. Dennis & T.E. Such, *Nickel and Chromium Plating*, Woodhead Publishing Limited, Cambridge, England, UK, 1993).
2. K.R. Newby, in *ASM Handbook, Volume 5*, S.R. Lampman (Ed.), ASM International, Materials Park, OH, 1994; p. 177.
3. T. Sahraoui, *et al.*, *J. Mater. Proc. Tech.*, **152** (1), 43 (2004).
4. B.D. Sartwell & P.E. Bretz, *Adv. Material Processes*, **157** (8), 25 (1999).
5. R.C. Tucker, Jr., in *ASM Handbook, Volume 5*, S.R. Lampman (Ed.), ASM International, Materials Park, OH, 1994; p. 497.
6. P.F. Ruggiero, *Adv. Material Processes*, **163** (7), 39 (2005).
7. J. A. Kubinski, *et al.*, *Plating & Surface Finishing*, **86** (10), 20 (1999).
8. B. Navinšek, P. Panjan & I. Milošev, *Surface & Coatings Technology*, **116-119**, 476 (1999).
9. D.W. Baudrand., in *ASM Handbook, Volume 5*, S.R. Lampman (Ed.), ASM International, Materials Park, OH, 1994; p. 290.
10. V.Y. Gertsman & R. Birringer, *Scripta Metallurgica et Materiala*, **30** (5), 577 (1994).
11. U. Klement, *et al.*, *Materials Science and Engineering A*, **203** (1-2), 177 (1995).
12. H. Natter, M. Schmelzer & R. Hempelmann, *J. Materials Research*, **13** (5), 1186 (1998).
13. M. Thuvander, *et al.*, *Mat. Sci. Technol.*, **17** (8), 961 (2001).
14. S. Eskin, *et al.*, *Plating & Surface Finishing*, **85** (4), 79 (1998).
15. K-L. Lin, *et al.*, *J. Materials Engineering and Performance*, **1** (3), 359 (1992).
16. T. Agladze, *et al.*, *Trans. Inst. Metal Finishing*, **75**, 30 (1997).
17. R. Mousavi, K. Raeissi & A. Saatchi, *Int'l. J. Modern Physics B*, **22** (18-19), 3060 (2008).
18. M. Donten, H. Cesiulis & Z. Stojek, *Electrochim. Acta*, **50** (6), 1405 (2005).
19. T. Nasu, *et al.*, *Materials Science & Engineering A*, **375-377**, 163 (2004).
20. A. Brenner, P. Burkhead & E. Seegmiller, *J. Research Nat'l. Bureau of Standards*, **39**, 351 (1947).
21. A. Brenner, *Electrodeposition of Alloys: Principles and Practice*, American Press Inc., New York, NY, 1963.
22. S. Oue, *et al.*, *J. Electrochem. Soc.*, **156** (1), D17 (2009).
23. M. Pisarek, M. Janik-Czachor & M. Donten, *Surface & Coatings Technology*, **202** (10), 1980 (2008).
24. A.S.M.A. Haseeb & K. Bade, *Microsystem Technologies: Micro- and Nanosystems Information Storage and Processing Systems*, **14** (3), 379 (2008).
25. O. Younes-Metzler, L. Zhu & E. Gileadi, *Electrochim. Acta*, **48** (18), 2551 (2003).
26. C.A. Schuh, T.G. Nieh & H. Iwasaki, *Acta Materialia*, **51** (2), 431 (2003).
27. M.D. Obradović, R.M. Stevanović & A.R. Despić, *J. Electroanal. Chem.*, **552**, 185 (2003).
28. T. Yamasaki, *et al.*, *Plating & Surface Finishing*, **87** (5), 148 (2000).
29. M. Obradović, *et al.*, *J. Electroanal. Chem.*, **491** (1-2), 188 (2000).
30. A.J. Detor & C.A. Schuh, *Acta Materialia*, **55** (12), 4221 (2007).
31. H. Hosokawa, *et al.*, *J. Materials Science*, **41** (24), 8372 (2006).
32. A. J. Detor & C.A. Schuh, *Acta Materialia*, **55** (1), 371 (2007).
33. A.J. Detor, M.K. Miller & C.A. Schuh, *Philosophical Magazine*, **86** (28), 4459 (2006).
34. ASTM B117-03: Standard Practice for Operating Salt Spray (Fog) Apparatus, ASTM International, W. Conshohocken, PA, 2003.
35. ASTM B537-70(2007): Standard Practice for Rating of Electroplated Panels Subjected to Atmospheric Exposure, ASTM International, W. Conshohocken, PA, 2007.
36. A.R. Jones, in *ASM Handbook, Volume 13B*, C. Moosbrugger (Ed.), ASM International, Materials Park, OH, 2005; p. 434.
37. A.R. Jones, in *Proc. AESF Chromium Colloquium*, NAFS, Washington, DC, 1994).

38. A. R. Jones, in *Proc. 4th International Colloquium on Chromium and Nickel Plating*, Ecole Nationale Supérieure des Mines de Saint-Etienne, Saint-Etienne, France, 2004.
39. G. Loar, K. Newby, B. Saas & H. Smith, Metal Finishing Suppliers' Association (NASF, Washington, DC).
40. M. Sisti & A. Ruffini, <http://www.pfonline.com/articles/pfd0507.html>, Gardner Publications, Cincinnati, OH, 2008.
41. A.J. Detor & C.A. Schuh, *J. Materials Research*, **22** (11), 3233 (2007).

About the authors



Jones



Hamann



Schuh

Dr. Allen R. Jones is a Product Expert - Functional Coatings and Lead Engineer - Product Commercialization at Xtallic Corporation. His primary interest is in improving the performance of functional electrodeposits and has 27 years of experience in surface engineering. Dr. Jones received his Ph.D. in Physical Chemistry from Rensselaer Polytechnic Institute in Troy, New York and a B.A. in Chemistry from Linfield College in McMinnville, Oregon.

Dr. Joseph A. Hamann has been a Senior Materials Engineer for four years at Xtallic. His research is focused on process development, including process scale-up, performance bench marking and materials characterization. He obtained his Ph.D. in 2006, M.S. in 2003, in Material Science, and in 2001 a B.S. in Material Science and Engineering, all from the University of Wisconsin, Madison.

Dr. Alan C. Lund co-founded Xtallic Corporation with Prof. Christopher Schuh, and is currently the Chief Technology Officer at Xtallic. Dr. Lund has degrees in Materials Science from the University of Illinois at Urbana-Champaign (B.S.) and Northwestern University (Ph.D.).

Dr. Christopher A. Schuh is the Danae and Vasilios Salapatias Associate Professor of Metallurgy, in the Department of Materials Science and Engineering at the Massachusetts Institute of Technology (MIT). He earned a B.S. degree in Materials Science and Engineering from the University of Illinois at Urbana-Champaign in 1997, and a Ph.D. in the same field from Northwestern University in 2001.

Shift Your Career into Overdrive

Getting the necessary education to launch or advance a successful career can be a daunting endeavor. The **AESF Foundation Home Study Programs** are designed to provide working adults and aspiring career professionals with the ability to get additional education quickly, conveniently and affordably. Courses are based around the course materials that you receive when you sign up for the program. The materials include lessons as well as homework. You will coordinate your study with the Technical Education Director of the Foundation, at your own pace. The Director will be your source to ask questions about the material, grade your homework and offer suggestions to improve your work.

Six new and improved education and training opportunities were launched in the past year to complement the numerous training opportunities already available. More will be offered as time progresses. The AESF Foundation is now pleased to offer the following home study options:

- [Electroplating and Surface Finishing - Parts 1 & 2](#)
(Each section of this course can be taken at different times)
- [Aluminum Finishing](#)
- [Chromium Plating for Engineering Applications](#)
- [Precious and Related Metals](#)
- [Wastewater Treatment and Control](#)

*[CLICK HERE TO DOWNLOAD A HOME STUDY APPLICATION](#)

